Simulation of Flame Acceleration and Deflagration to Detonation Transition in Components of Chemical Plants

Christoph Wieland, Christoph Hirsch, Thomas Sattelmayer
Chair of Thermodynamics, Technical University Munich, 85748 Garching, Germany
Florian Scharf, Vera Hoferichter, Hans-Peter Schildberg
BASF SE, Ludwigshafen, Germany

1 Introduction

Risk analysis is a central aspect of plant design in the chemical and process industry as potentially hazardous mixtures are involved in the production (cf. [7], [8]). The most important aspect is the protection of life and environment in the event of an accident. In addition, economic factors, such as the avoidance of expensive production losses, also play a role. Comprehensive analysis must always consider a huge variety of accident scenarios. The ignition of a flammable mixture during an accident can create conditions that lead to a deflagration-to-detonation transition (DDT) which can cause severe damage to the structures due to extremely high pressure loads [7].
The wide variety of mixtures, geometries and process conditions does not allow for an experimental investigation of whether a DDT can to be expected in a given plant section. Therefore, risk analysis has to rely on reference experiments and best practice estimation methods to assess the DDT risk in the individual case. That is why the methods at BASF are extended to include a CFD-solver capable of simulating the whole process of run-up to a detonation. A hybrid pressure-/density-based solver based on the works of Ettner [2] and Hasslberger [3] is presented in this work. It uses the OpenFOAM package [9] and is capable of simulating flame acceleration and DDT of $H_2/O_2/N_2$ and $C_2H_4/O_2/N_2$ mixtures in smooth pipes and spheres. To allow its application in industry, reasonably short calculation runtimes are needed which is achieved by using under-resolved grids. As a consequence, essential physical phenomena have to be modelled. This work highlights the solver structure and the key models used. Additionally some validation results are shown. As a chemical plant consists of various components, smooth pipes and a 20 l sphere were considered. Therefore, two different types of flame propagation: quasi 1-D propagation in the smooth pipes and 3-D propagation in the sphere are used to validate the CFD-solver.

2 Solver Architecture

In this section, the numerical method of the hybrid solver is outlined. Since flame acceleration and DDT are highly transient phenomena, the DDT solver is based on the unsteady compressible Favre Averaged Navier-Stokes equations, using the ideal gas law. Two transport equations for the internal total energy were found necessary to capture the unburnt and burnt state properly. Turbulence is considered by the

Correspondence to: wieland@td.mw.tum.de

$k-\omega$ SST model [5]. Wall functions are used to reproduce turbulence production in the boundary layer, crucial for the early stage of flame acceleration in smooth pipes. Moreover, adaptive mesh refinement (AMR) is applied to the wall boundary area in order to remain within the range of validity of the wall functions used. Activation of the AMR is controlled by local velocity gradients in the boundary area. Flame propagation is described by an equation for reaction progress variable as described in more detail in the next section. Also a flame wrinkling transport equation must be solved to capture the transient effects as outlined below. For the activation of the detonation source term, a transport equation for the dimensionless ignition delay time τ is needed.
A hybrid pressure-/density-based architecture is used to capture both deflagrative flame acceleration as well as DDT and detonation propagation. The initial acceleration phase is captured by the pressure-based solver, as this phase can be considered incompressible. This became necessary as the density-based solver captured the pressure rise and the related creation of a flow field and turbulent boundary layer ahead of the flame insufficiently during this stage of flame acceleration. With increasing flame and flow velocities, however, the density-based solver is better suited. Therefore, a transition criterion was developed for the switch from the pressure- to density-based solution of the equations. Two criteria are used depending on the type of flame propagation as shown in Fig. 1. In pipe-like geometries skeched on the left the flame propagation is quasi one-dimensional and flame acceleration is dominated

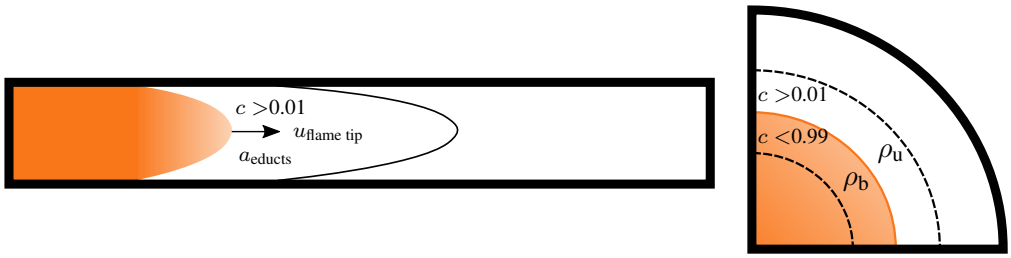

Figure 1: Transition criterion between pressure- and density-based solver architecture. Flame Ma number criterion for smooth tubes on the left and expansion ratio criterion for spheres on the right.

by turbulent flame wrinkling. Here a flame Ma number (Ma = $u_{\text{flame tip}}/a_{\text{educts}}$) compares the flame-tip velocity with the speed of sound of the educts ahead of the flame. If a threshold of unity is exceeded, the flame is considered a fast flame and the transition to the density-based solution is initiated. In spherical geometries, where flame propagation takes place in all directions and expansion of the reaction products as well as growth of the flame surface are crucial for flame acceleration, an average expansion ratio over the flame front $\sigma = \rho_{\text{u}}/\rho_{\text{b}}$ is calculated as transition criterion. If a critical value defined by the expansion ratio of the initial state and a fuel dependent factor $\sigma_{\text{trans}} = \sigma_{\text{initial}}\text{-}\alpha_\sigma$ is exceeded, transition is realised. This hybrid solver architecture allows for a very efficient computation.

3 Combustion Modelling

In this section the combustion models for $H_2/O_2/N_2$ and $C_2H_4/O_2/N_2$ mixtures are briefly described. A more detailed description and validation of the model is given in [11].
Flame propagation is represented by the reaction progress variable (c) approach [6]. In the under-resolved context and with a focus on computational efficiency it is the methodology of choice since only one transport equation needs to be solved, which is given by

$$\frac{\partial}{\partial t}\left(\overline{\rho}\tilde{c}\right) + \frac{\partial}{\partial x_j}\left(\overline{\rho}\tilde{u}_j\tilde{c}\right) = \frac{\partial}{\partial x_j}\left[\left(\overline{\rho}\mathrm{D}_{\text{eff}}\right)\frac{\partial \tilde{c}}{\partial x_j}\right] + \max\left(\dot{\omega}_{\text{def}}, \dot{\omega}_{\text{det}}\right). \tag{1}$$

The fresh-gas state is defined by $c = 0$ and the burnt state by $c = 1$. Intermediate states are linearly interpolated using c and lookup tables for the fully burnt state. These tables are derived from 0-D reactor calculations for various fuel contents, temperatures and pressures. Modelling refers to the source term in Eqn. 1, which is given by the maximum of a deflagration and a detonation source term.

3 Deflagration Source Term

The deflagration source term is defined as

$$\dot{\omega}_{\text{def}} = \overline{\rho}_{\text{u}} \text{G} \text{S}_{\text{t}} \left| \frac{\partial \tilde{c}}{\partial x_j} \right|. \tag{2}$$

Here ρ_{u} is the unburnt density, G considers quenching according to the model of Zimont [12] and S_{t} represents the turbulent burning velocity. In terms of hydrogen mixtures, S_{t} is calculated according to the model of Katzy [4] while for ethylene mixtures, the correlation from Dinkelacker [1] is used:

$$\text{S}_{\text{t}} = \begin{cases} \text{S}_{\text{l}} \Xi_{\text{inst}} \text{F}_{\text{pressure}} \text{F}_{\text{stretch}} \Xi_{\text{turb}} \text{F}_{\text{grid}} \text{F}_{\text{enclosure}} & \text{for Hydrogen} \\ \text{S}_{\text{l}} \Xi & \text{for Ethylene.} \end{cases} \tag{3}$$

In the Dinkelacker correlation [1] for ethylene mixtures, Ξ includes flame wrinkling due to instabilities and turbulence as well as a pressure dependence. To capture the temporal development of the turbulence field and flame wrinkling both Ξ form Dinkelacker and Ξ_{turb} from Katzy are used as the equilibrium source term of the flame wrinkling transport equation of Weller [10]. If only algebraic models are used, they cause overestimation of the instantaneous flame wrinkling.

3.1 Detonation Source Term

Detonation is modelled by a two-step mechanism, which includes a phase of ignition delay before significant auto-ignition effects take place, and a subsequent heat release according to the following quadratic function:

$$\dot{\omega}_{\text{det}} = \theta \frac{2\text{B}}{\text{t}_{\text{exo}}} c \left(1 - c\right) \text{H} \left(\tau - 1\right) \text{H} \left(\text{T} - \text{T}_{\text{Trans}}\right). \tag{4}$$

B is a model constant, and θ (pressure criterion) as well as the temperature criterion Heavyside side function $\text{H} \left(\text{T} - \text{T}_{\text{Trans}}\right)$ are used to model the von Neumann peak, which cannot be resolved on the under-resolved grids. For that purpose, T_{Trans} is set to the temperature at the von Neumann peak, which is tabulated according to fuel content, unburnt temperature and pressure, taking into account preconditioning of the fresh gas. The dimensionless parameter τ considers the phase of ignition delay by comparing the actual simulation time with tabulated ignition-delay times $\tau = \frac{\text{t}}{\text{t}_{\text{ign(x,Tu,p)}}}$. To consider the temporal evolution, a transport equation is solved for τ. If τ becomes unity, the ignition-delay time has expired and $\text{H} \left(\tau - 1\right)$ becomes unity, at which point the detonation source term is activated.
The timescale of the detonative reaction t_{exo} is calculated as

$$\text{t}_{\text{exo}} = \left(1 - c\right) \frac{\left(\triangle\right)^{\frac{1}{3}}}{\text{D}_{\text{CJ}}}. \tag{5}$$

t_{exo} describes the time needed by the detonation complex to pass a cell, and is therefore calculated using the local characteristic cell size $\triangle$, derived from the volume, and the Chapman-Jouguet velocity D_{CJ}. Already burnt parts of a cell are taken into account by the factor $\left(1 - c\right)$. D_{CJ} is tabulated in terms of fuel content, unburnt temperature and pressure in order for preconditioning to be considered.

4 Results and Validation

To simulate the smooth pipe cases, a quarter of the pipe is computed. Hence, symmetry boundary conditions are applied. The initial grid size is set to 2.0 mm, resulting in 400,000 cells for a pipe with a diameter of 43.1 mm and a length of 9.48 m. Level 1 refinement with two buffer layers is used for the AMR. Typical runtime is 30h on 16 cores of a Linux workstation.
Regarding the 20 l sphere with a diameter of 340 mm, an eighth is simulated and associated symmetry boundary conditions are applied. Grid size is also set to 2.0 mm, leading to 330,000 cells. No AMR is used. Typical runtime is 24h on 16 cores of a Linux workstation.

4.1 Smooth Pipes

For smooth pipes the CFD results are validated based on the prediction of the experimental DDT locations. Due to the small number of repetitions of the individual experiments, statistics cannot be captured, so the target of a successful prediction is set to lie within a confidence interval of +/- 25 % of the experimental. The experimental DDT locations from Schildberg ([7], [8]) are obtained from the locus of the maximum plastic deformation of the pipe which can be directly related to maximum pressure load. Therefore, the position of maximum pressure along the wall is recorded for validation. Also flame-tip position data from measurements recently taken at BASF are available.
Fig. 2 illustrates the comparison between simulated (red line) and experimental (black line with dots) flame-tip position data on the left, and flame tip-tip velocities on the right. The transition between pressure- and density-based solver took place at 6.01 ms. Good agreement between simulation and ex-

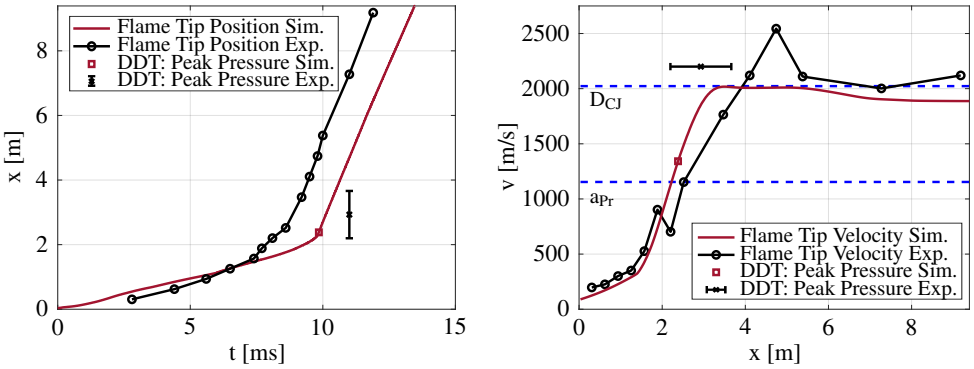

Figure 2: Comparison of flame-tip position data on the left and flame-tip velocity data on the right for a stoichiometric $H_2/O_2/N_2$ mixture with 29.56 Vol.-% H_2 (case 2 in [7]) at 12 bar and 293 K.

periment can be observed. The flame accelerates continuously up to 2.27 m, where a kink can be seen in the flame-tip position data, indicating the occurence of significant self-ignition effects. DDT in terms of maximum pressure load is observed directly afterwards, and can be predicted within the confidence interval of the experimental DDT at 2.93 m. In the subsequent detonative regime, there is a linear dependence of the flame-tip position on time, which is characteristic of stable detonation propagation at a constant speed. There is a delay in the simulative flame-tip position data as the experimental timescales are overpredicted, which can be attributed primarily to deficits in the ignition modelling on the underresolved grids. Correspondingly, the flame-tip velocity data shows continuous acceleration and a strong increase due to the aforementioned self-ignition effects. DDT occurs when the flame reaches a velocity in the order of the speed of sound of the reaction products a_{Pr}, which is considered a necessary criterion for DDT to take place. Afterwards, the flame reaches D_{CJ} and relaxes to a value slightly below this, while propagating along the tube.

Fig. 3 shows flame-tip position over time on the left and flame-tip velocity over position on the right for a stoichiometric $C_2H_4/O_2/N_2$ mixture with 9.33 Vol.-% C_2H_4. Only the experimental DDT location [8] is available for validation. Transition between pressure- and density-based architecture took place at 7.92 ms. The overall propagation behaviour is identical to Fig. 2, including continuous deflagrative flame acceleration, the characteristic kink and detonation propagation at a constant speed. DDT can again be predicted within the confidence interval of the experimental DDT at 1.68 m.

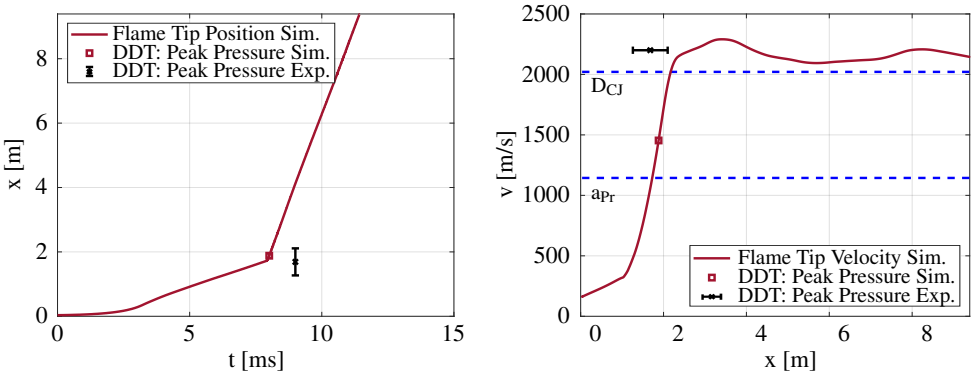

Figure 3: Comparison of flame-tip position data on the left and flame-tip velocity data on the right for a stoichiometric $C_2H_4/O_2/N_2$ mixture with 9.33 Vol.-% C_2H_4 (case 12 in [8]) at 8 bar and 293 K.

4.2 20 l Sphere

Validation is carried out by means of the pressure traces for mixtures of 9.33 Vol.-% C_2H_4 and 10.0 Vol.-% C_2H_4 in Fig. 4. Pressure data is shifted in time to match the experimental data. Transition between the solver architectures took place at 5.12 ms and 4.85 ms, respectively. Good agreement between simulation and experiment can be observed. The experimentally determinded boundary between deflagrative and detonative explosions for stoichiometric ratios of C_2H_4:O_2 with varying oxygen contents can be reproduced by the simulation. Regarding the 9.33 Vol.-% C_2H_4 mixture no DDT occurs, indicated by the small pressure oscillations. However, looking at the 10.0 Vol.-% C_2H_4 mixture, DDT can be observed,

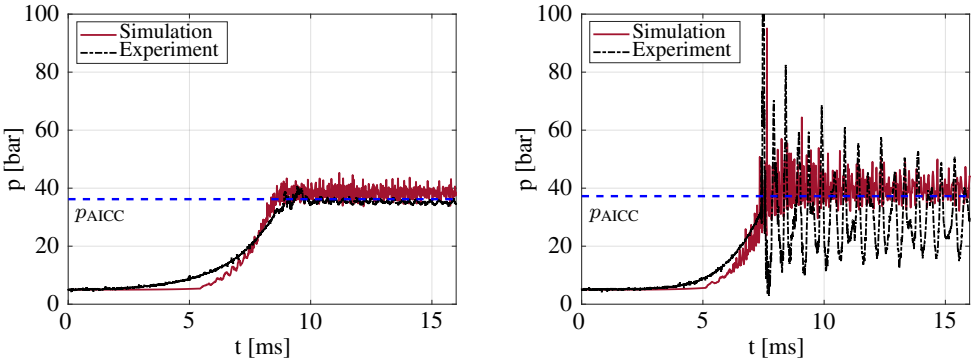

Figure 4: Comparison of pressure data for two stoichiometric $C_2H_4/O_2/N_2$ mixtures with 9.33 Vol.-% C_2H_4 (left) and 10.0 Vol.-% C_2H_4 (right) at 5 bar and 473 K. Adiabatic, isochoric explosion pressure (p_{AICC}) added by blue dashed line.

denoted by strong pressure peak at 7.5 ms and strong oscillations. Moreover, the averaged pressure data for both simulation and experiment match the adiabatic isochoric explosion pressure (p_{AICC}).

In conclusion, the presented DDT solver with a hybrid pressure-/density-based solver architecture has proven to be a robust and efficient tool for industrial application, which allows various accident scenarios in components of chemical plants to be analysed. The global propagation behaviour and DDT location can be predicted correctly. In addition, critical conditions for DDT could be identified successfully.

Acknowledgement

The presented work is funded by the BASF SE, whose support is gratefully acknowledged.

References

[1] Muppala Reddy, S., Naresh, K., Dinkelacker, F., Leipertz, A. (2004). Development of an algebraic reaction rate closure for the numerical calculation of turbulent premixed methane, ethylene and propane/air flames for pressure up to 1.0 MPa. Comb. and Fl. 140: 257-266

[2] Ettner, F. (2013). Effiziente numerische Simulation des Deflagrations-Detonations-Übergangs. PhD Thesis Technische Universität München

[3] Hasslberger, J. (2017). Numerical Simulation of Deflagration-to-Detonation Transition on Industry Scale. PhD Thesis Technische Universität München

[4] Katzy, P. (2020). Combustion Model for the Computation of Flame Propagation in Lean Hydrogen-Air Mixtures at Low Turbulence. PhD Thesis Technische Universität München

[5] Menter, F. (1994). Two-equation eddy-viscosity turbulence models for engineering applications.. AIAA J. 32: 1598-1605

[6] Poinsot, T., Veynante, D. (2005). Theoretical and numerical combustion. RT Edwards Inc.

[7] Schildberg, H.-P. (2015). Experimental determination of the static equivalent pressures of detonative explosions of stoichiometric H2/O2/N2-mixtures in long and short pipes. Proc. of the ASME 2015 Pressure Vessels and Piping Conference

[8] Schildberg, H.-P. (2018). Experimental determination of the static equivalent pressures of detonative explosions of ethylene/O2/N2-mixtures and cyclohexane/O2/N2-mixtures in long and short pipes. Proc. of the ASME 2018 Pressure Vessels and Piping Conference

[9] Weller, H., Tabor, G., Jasak, H., Fureby, C. (1998). A tensorial approach to computational continuum mechanics using object-oriented techniques. Comp. in Phy. 12:620-631

[10] Weller, H. (1993). The development of a new flame area combustion model using conditional averaging.

[11] Wieland, C., Scharf, F., Schildberg, H.-P., Hoferichter, V., Eble J., Hirsch, C., Sattelmayer, T. (2021). Efficient simulation of flame acceleration and deflagration-to-detonation transition in smooth pipes. J. of Loss Prev. 71

[12] Zimont, V. (2000). Gas premixed combustion at high turbulence. Turbulent flame closure combustion model. Exp. Therm. and Fl. Sc. 21: 179-186